ACS APPLIED MATERIALS & INTERFACES

Letter

www.acsami.org

Highly Efficient Bilayer Interface Exciplex For Yellow Organic Light-Emitting Diode

Wen-Yi Hung,*[,†] Guan-Cheng Fang,[†] Yuh-Chia Chang,[‡] Ting-Yi Kuo,[‡] Pi-Tai Chou,*[,‡,§] Shih-Wei Lin,[‡] and Ken-Tsung Wong*[,‡,⊥]

[†]Institute of Optoelectronic Sciences, National Taiwan Ocean University, Keelung 20224, Taiwan

[‡]Department of Chemistry and [§]Center for Emerging Material and Advanced Devices, National Taiwan University, Taipei 10617, Taiwan

[⊥]Institute of Atomic and Molecular Sciences, Academia Sinica, Taipei, 10617, Taiwan

Supporting Information

ABSTRACT: A simple three-layer interfacial-type yellow emission exciplex device with an external quantum efficiency as high as 7.7% has been successfully achieved by combining conformation compatible C_3-symmetric hole-transporting TCTA and electron-transporting 3P-T2T. The excellent and balanced charge-transporting properties of TCTA and 3P-T2T and the large energy-levels offset (0.8 eV) of TCTA/3P-T2T interface play important roles for the efficient exciplexes formation, which are effectively confined around the interfacial region due to the high triplet energies (2.85 eV) of TCTA and 3P-T2T. The high-performance OLED was believed to be from the effective harvest of exciplex triplet excitons via reverse intersystem crossing process.

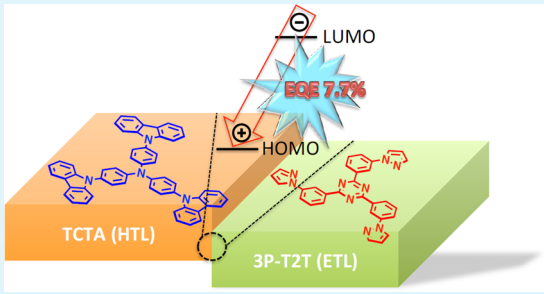

KEYWORDS: *organic light-emitting diode (OLED), time-of-flight, exciplex, bilayer interface, reverse intersystem crossing (RISC), C_3-symmetry*

INTRODUCTION

The new display technologies based on organic light-emitting diode (OLED) have started to benefit our daily life. Since the first discovery of thin-film based OLED by Tang and Van Slyke,[1] tremendous endeavors have been made to pursue the strategies for efficient extraction of light from the electro-generated emissive excitons. One of the most important focuses to date is to recover the 75% triplet exciton, which is typically nonemissive in organic emitters. Fortunately, the selection rule forbidden process can be relaxed by the strong spin−orbit coupling effect induced by heavy metals such as Ir, Os, Pt, and Cu, giving the cornerstone of commercialized active matrix OLEDs (AM-OLED) display nowadays. However, the scarcity of metal resources and hence the concern of future production cost may shadow the prospects of metal-based phosphorescence AM-OLEDs. New tactics to harvest the triplet excitons from potentially more cost-competitive pure organic emitters are therefore highly desired. Recently, two upconversion mechanisms including triplet−triplet annihilation (TTA)[2−5] and thermally activated delay-fluorescence (TADF)[6−11] have been successfully utilized to yield high efficiency OLEDs with tailor-made pure organic emitters. As compared to TTA, which can lead to a theoretical maximum 62.5% of internal quantum efficiency (IQE),[3] the achievable 100% IQE of TADF-based OLEDs may receive more future interests.

The success of TADF relies on the small energy difference (ΔE_{ST}) between the singlet (S_1) and triplet (T_1) excited states, resulting in an efficient reverse intersystem crossing (RISC) (i.e., from T_1 back to S_1). Therefore, the electro-generated nonemissive triplet manifold can be relaxed back to the S_1 state to give a high IQE. Normally, molecules capable of demonstrating TADF are composed of structurally weak-coupled electron donor (D) and acceptor (A) components, leading to an intramolecular charge transfer (ICT) behavior. The design of a new D/A molecule to attain efficient TADF is nontrivial, which requires the subtle harnessing on the degree of ICT within the molecular framework. Alternatively, the excited states with small ΔE_{ST} can also be achieved by the formation of exciplex via intermolecular charge transfer between physically blended electronic donor and acceptor molecules. The exciplex applications in OLEDs have been realized and fast booming. With the judicious selection of donor and acceptor materials, OLEDs with exceptionally high electroluminescence (EL) efficiencies have been successfully achieved recently.[12−27] The EL efficiency of exciplex depends on the yields of exciplex exciton, which correlate with the interaction between donor and acceptor molecules. Considering that the electron transfer takes place between the donor and acceptor molecules, compact intermolecular contact by mixing donor and acceptor molecules as an emitting layer (a single-

Received: May 28, 2013
Accepted: July 12, 2013
Published: July 12, 2013

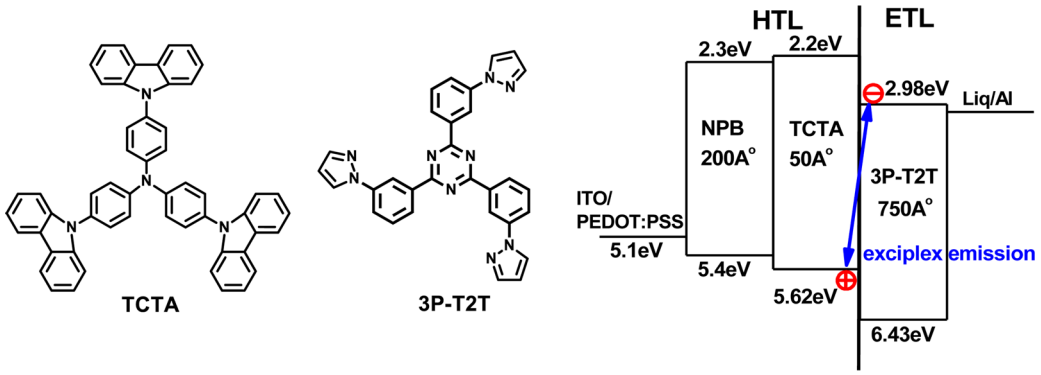

Figure 1. (a) Molecular structures of TCTA and 3P-T2T. (b) Scheme of exciplex emission formed between TCTA and 3P-T2T with HOMO and LUMO levels.

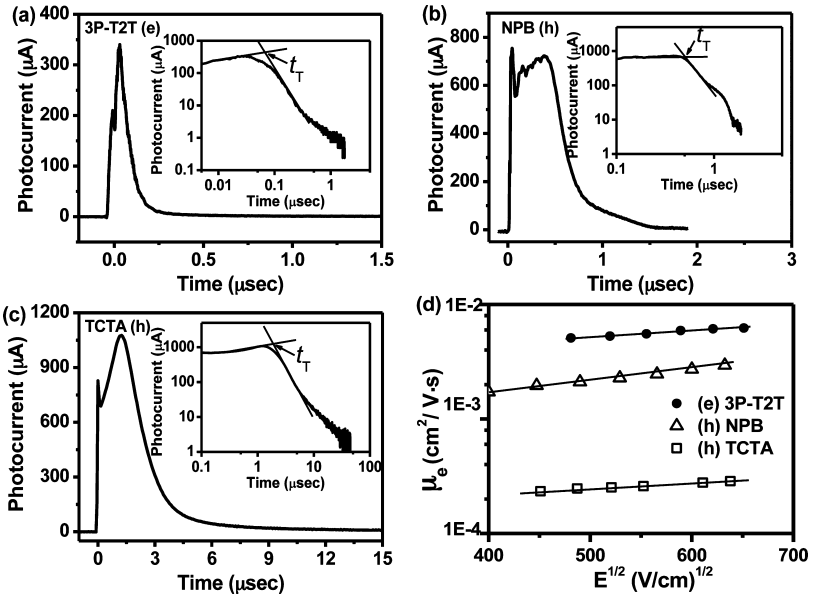

Figure 2. Representative TOF transient photocurrent signals for (a) electrons of 3P-T2T at $E = 3.9 \times 10^5$ V cm^{-1}; (b) holes of NPB at $E = 2.4 \times 10^5$ V cm^{-1} ; (c) holes of TCTA at $E = 3.1 \times 10^5$ V cm^{-1} and insets are the double logarithmic plots. (d) Carrier mobility of compounds plotted with respect to $E^{1/2}$.

layer type) has been exploited ubiquitously in the exciplex-based OLEDs.[12−20] In yet another approach, the external quantum efficiencies (EQE) of previously reported exciplex-emitting devices from the interfacial layer (a bilayer type) between donor and acceptor materials are far from satisfactory.[21−27] This leads us to mull the possibility over the exciplex formation in the interface between two individual donor and acceptor layers, so that the fabrication of the devices can be well organized under a rational and engineering basis. The EL efficiency of a bilayer-type exciplex can be significantly improved by employing an appropriate combination of donor and acceptor based on the following criteria: (1) The donor and acceptor possess high hole and electron mobility, respectively, allowing sufficient charge carriers reaching to the interface. (2) The charge carriers can be accumulated at the interfacial region due to the large differences between the frontier energy levels of donor and acceptor, giving a high propensity of electron−hole recombination to generate S_1 and T_1 states. (3) More importantly, the triplet energies (E_T) of donor and acceptor need to be higher than that of the exciplex for confining the electro-generated triplet state within the interfacial region. Consequently, the nonemissive T_1 state can predominantly shuttle back to emissive S_1 state, leading to a high-efficiency bilayer-type exciplex OLED.

In this communication, we report a bilayer-type exciplex OLED by combining hole-transporting 4,4′,4″-tri(N-carbazolyl)triphenylamine (TCTA) as donor and 2,4,6-tris(3-(1H-pyrazol-1-yl)phenyl)-1,3,5-triazine (3P-T2T)[28] as acceptor. The high efficiency is attributed to the high and balanced hole and electron mobilities of TCTA and 3P-T2T, respectively, and the large energy-levels offsets at the TCTA/3P-T2T interface, where the accumulated charge carriers recombine to give emissive exciplex excitons efficiently. The electro-generated exciplex is effectively confined within the interfacial region due to the high E_Ts of TCTA and 3P-T2T, rendering a leaping improvement on the light-emitting efficiency via a RISC process. Unlike most of recent reports on exciplex-based OLEDs via compact intermolecular contact,[16,17] i.e., mixing electron donor and acceptor materials, our study presents an efficient exciplex generation from the interface of a bilayer structure. This finding is of great importance, which provides an excellent opportunity to fine-tune parameters in a rational and engineering basis. As a result, using a simple three-layer interfacial-type exciplex device, an

dx.doi.org/10.1021/am402032z | ACS Appl. Mater. Interfaces 2013, 5, 6826−6831

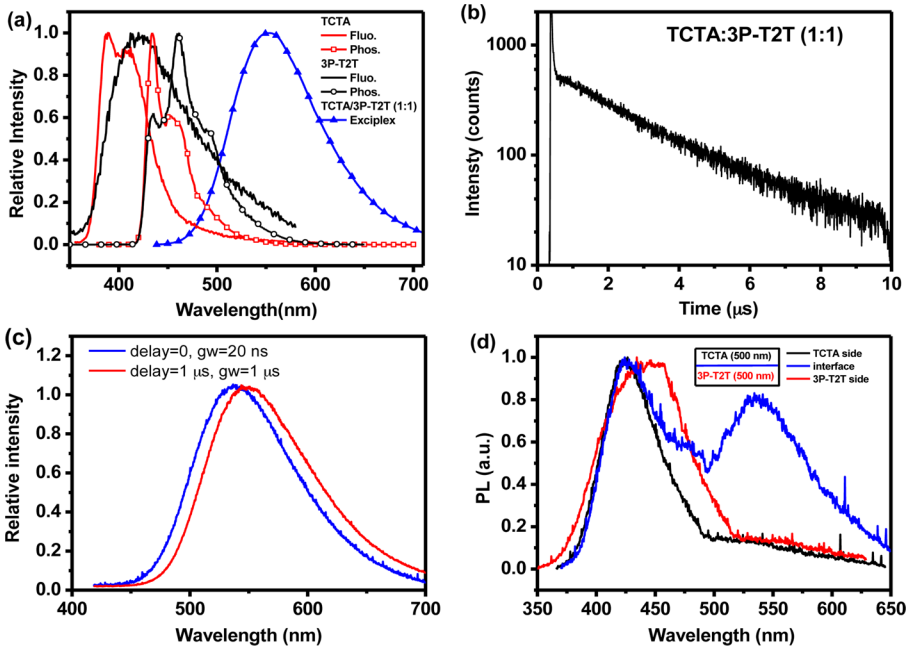

Figure 3. (a) Steady-state fluorescence spectra (PL) of TCTA and 3P-T2T neat films and TCTA/3P-T2T (1:1) mixed film at 300 K, and phosphorescence spectra (Phos.) of TCTA and 3P-T2T in a 77 K EtOH glass matrix. (b) The decay dynamics of the exciplex emission for the TCTA/3P-T2T mixture film, monitored at 550 nm. (c) The prompt (delay = 0, gate width = 20 ns) and delay (delay = 1 μs, gate width = 1 μs) in TCTA/3P-T2T mixture film (d) Two separated TCTA and 3P-T2T layers (~500 nm thickness for each) stacked together. The emission was acquired at various positions of the cross section along the bilayer by a microscope optical detecting system with ~350 nm spatial resolution (λ_{ex} = 355 nm): the TCTA layer (black), the 3P-T2T layer (red line), and the interface area (blue).

external quantum efficiency (EQE) as high as 7.7% has been achieved.

RESULTS AND DISCUSSION

The molecular structures of TCTA and 3P-T2T are shown in Figure 1. Interestingly, some of reported TADF-active molecules consist of carbazole as donor component and triazene as acceptor unit not only because of their unique electronic properties but also their respective high E_Ts.[6,7] Since we aimed at a small ΔE_{ST} for an exciplex via intermolecular charge transfer, it would be reasonable to select the donor and acceptor containing with the structures of carbazole and triazene, respectively, to afford exciplex efficiently. More importantly, the C_3-symmetry feature of TCTA and 3P-T2T may provide better conformational compatibility for effective intermolecular contact, a crucial factor for the exciplex formation.[29,30] Figure 1 also shows a schematic energy diagram of TCTA and 3P-T2T, in which the highest occupied molecular orbital (HOMO) energies of TCTA and 3P-T2T were determined by photoelectron yield spectroscopy (Riken AC-2) (see Figure S1 in the Supporting Information) and ultraviolet photoelectron spectroscopy (UPS),[28] respectively. The lowest unoccupied molecular orbital (LUMO) levels were then calculated with the optical band gap determined from their absorption spectra. Obviously, the high LUMO of TCTA and the low HOMO of 3P-T2T lead to large band-edge offsets (ca. 0.8 eV) at the TCTA/3P-T2T interface, giving a great ability for gathering charge carriers. As the energy-level offsets are larger than the binding energy of organic semiconductors,[31,32] the photon energy of the exciplex emission can be directly correlated to the energy difference between the HOMO of TCTA and the LUMO of 3P-T2T without prior injection of a charge carrier into the opposite material.

The intensity of exciplex emission relies on the charge carriers density accumulated at donor/acceptor interface, which in turn determines the device efficiency. Hence, high carrier mobilities of donor/acceptor play an important role in highly efficient exciplex-based OLEDs.[19] In the earlier attempt we were unfortunately unable to measure the electron mobility of 3P-T2T by traditional time-of-flight (TOF) technique.[28] In this study, alternatively, we employed an ambipolar oligofluorene (E3) as the charge-generation layer in the TOF mobility measurements[33] and successfully measured the electron mobility of 3P-T2T (Figure 2). The electron mobility of 3P-T2T is in the range from 5.1×10^{-3} to 6.2×10^{-3} cm^2 V^{-1} s^{-1} for fields varying from 2.3×10^5 to 4.2×10^5 V cm^{-1}. Such high electron mobility of 3P-T2T is comparable with the highest one among the ETMs ever reported.[34,35] In addition, we also evaluated the hole mobility of NPB and TCTA with TOF technique, the result of which gave hole mobility of NPB in the range from 9.4×10^{-4} to 1.4×10^{-3} cm^2 V^{-1} s^{-1} for fields varying from 2.0×10^5 to 4.5×10^5 V cm^{-1} and TCTA in the range from 2.3×10^{-4} to 2.9×10^{-4} cm^2 V^{-1} s^{-1} for fields varying from 2.0×10^5 to 4.1×10^5 V cm^{-1}. Obviously, the electron mobility of 3P-T2T (ETL) is higher than that of the hole mobility of NPB/TCTA (HTL) and can thus quickly transport electrons to the interface.

Figure 3a displays the photoluminescence (PL) spectra of pristine TCTA and 3P-T2T films, and TCTA/3P-T2T (1:1) mixed film, whereas the absorption (Abs) spectra of these films are also shown in Figure S2 (see the Supporting Information). Obviously, the resulting PL spectrum of TCTA/3P-T2T centered at ~544 nm is red-shifted by 155 and 124 nm relative to the emission peak wavelength of TCTA and 3P-T2T, respectively. According to the band gap arrangement, it is reasonable to assign this anomalous emission originating from an exciplex formed between the electron donor TCTA and the

dx.doi.org/10.1021/am402032z | ACS Appl. Mater. Interfaces 2013, 5, 6826−6831

electron acceptor 3P-T2T. The photon energy of the exciplex obtained from the onset (472 nm) of the emission is derived to be 2.63 eV, which is in good agreement with the difference (2.64 eV) between the HOMO of TCTA (−5.62 eV) and the LUMO of 3P-T2T (−2.98 eV). Supplementary support of the assignment is also provided by the dynamics of relaxation of the exciplex emission monitored at 550 nm in Figure 3b, in which the decay is composed of a prompt fluorescence of ∼4.2 ns and a long delayed fluorescence of 2.4 μs. Figure 3c reveals the prompt dominant (delay = 0, gate width = 20 ns) and delayed (delay = 1 μs, gate width = 1 μs) fluorescence spectra. The slight energy difference of <0.2 kcal/mol between two emission peaks, in a qualitative manner, reflects the small energy gap between exciplex singlet and triplet states due mainly to the lack of electron correlation and hence rather small electron exchange integral.[36] According to their respective phosphorescence shown in Figure 3a, the triplet state (T_1) energy levels for both TCTA and 3P-T2T are calculated to be coincidently ca. 2.85 eV, which are apparently higher than that of the exciplex emission. The result guarantees the confinement of the triplet-state exciplex within the interface.

To gain in-depth insight into the exciplex formation, we then made further attempts to investigate the exciplex formation in the interface between two separated TCTA and 3P-T2T layers, which are prepared by vacuum deposition sequentially. The emission was then acquired at various positions along the cross section of the double layers by an optical microscope detecting system (∼350 nm spatial resolution, λ_{ex} = 355 nm) incorporated with an intensified charge coupled detector (ICCD). Because of the relatively low optical resolution, each layer was intentionally prepared to be as thick as ∼500 nm for this study. The resulting emission spectra shown in Figure 3d are remarkable. Upon excitation at the TCTA (or 3P-T2T) layer from the cross section, the spectral profile is dominated by the individual TCTA (or 3P-T2T) emission. In sharp contrast, excitation at the interfacial area results in a distinct exciplex emission band maximized at 544−550 nm. Note that upon probing the interfacial layer, certain interfering TCTA and 3P-T2T prompt fluorescence from TCTA and 3P-T2T layers, respectively, is unavoidable because of the limit of spatial resolution. Likewise, the contamination of exciplex emission is non-negligible upon monitoring the emission at each TCTA or 3P-T2T layer, shown in Figure 3d. Nevertheless, because of the very different relaxation dynamics, the exciplex emission from the interfacial area can be resolved by the spectral temporal evolution shown in Figure 4, where the exciplex emission becomes a sole component after a delay time of, for example, 250 ns.

Standing on the above PL results, namely that the exciplex emission can be efficiently generated from the interface between donor and acceptor layers, our first attempt is to employ a relatively simple configuration for fabricating interfacial (bilayer-type, device I) exciplex device OLED devices: ITO/polyethylene dioxythiophene: polystyrene sulfonate (PEDOT:PSS, 30 nm)/4,4′-bis[*N*-(1-naphthyl)-*N*-phenyl]biphenyldiamine (NPB, 20 nm)/ 4,4′,4″-tri(N-carbazolyl)triphenylamine (TCTA, 5 nm)/ 3P-T2T (75 nm)/ Liq (0.5 nm)/Al; NPB/TCTA functioned as the HT layers, whereas 3P-T2T functioned as ETL. Because of the large band-edge offsets (ca. 0.8 eV) at TCTA/3P-T2T interface, holes and electrons are transported through TCTA and 3P-T2T to accumulate at the interface (Figure 1). The trapping of the exciton at the interface to form exciplex emission here provides

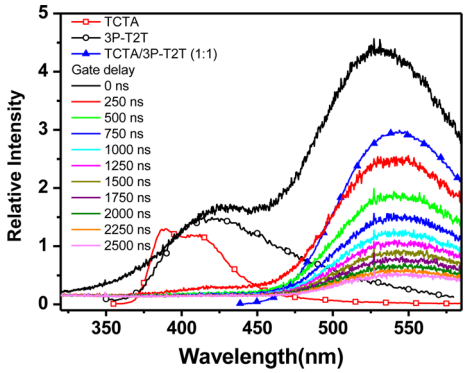

Figure 4. Spectral temporal evolution of the emission probed at the interfacial section between TCTA and 3P-T2T layers with various delay times shown in inset. Also shown are the emission spectra from TCTA and 3P-T2T neat films. For a fair comparison the exciplex emission of a mixture of TCTA/3P-T2T (1:1) film is also depicted. See text for the detailed elaboration.

direct evidence for the EL spectra. For comparison, an exciplex device (device II) was also fabricated by inserting a mixture layer (25 nm) of TCTA and 3P-T2T with ratio of 1:1 between TCTA/3P-T2T interface.

Figure 5 depicts the current density−voltage−luminance (J−V−L) characteristics, device efficiencies, and EL spectra of the devices. The key characteristics of devices are summarized in

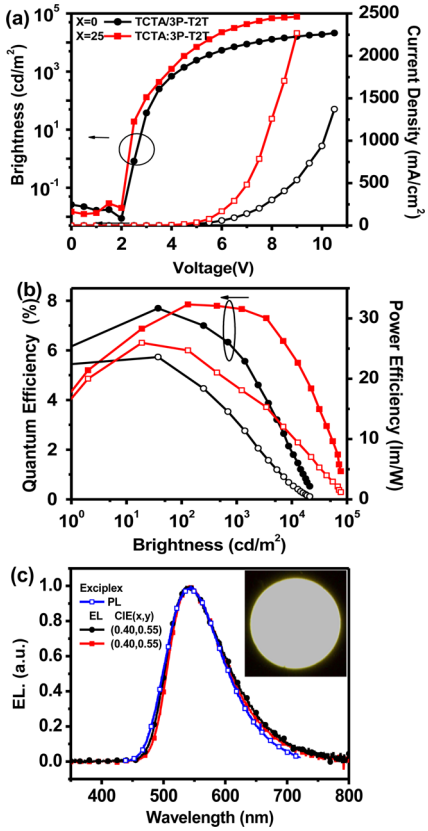

Figure 5. (a) Current density−voltage−luminance (J−V−L) characteristics. (b) External quantum (EQE) and power efficiencies (PE) as a function of brightness. (c) EL spectra of devices with the structure ITO/pedot:pss (30 nm)/NPB (20 nm)/TCTA (5 nm)/ TCTA: 3P-T2T 50 mol % (X nm)/ 3P-T2T (75-X nm)/Liq/Al, where X = 0 and 25.

dx.doi.org/10.1021/am402032z | ACS Appl. Mater. Interfaces 2013, 5, 6826−6831

Table 1. EL Performance of Exciplex Devices

device	X^a (nm)	$V_{on}{}^b$ (V)	^{c}at 1000 cd m^{-2} (V, %)	L_{max} (cd m^{-2}, V)	I_{max} (mA cm^{-2})	EQE^d (%)	CE^e (cd A^{-1})	PE^f (lm W^{-1})
I	0	2.0	4.2, 6.0	21100, 10.5	1370	7.7	22.5	23.6
II	250	2.0	3.8, 7.7	77100, 9.0	2270	7.8	23.6	26.0

[a]The thickness of TCTA:3P-T2T (1:1) mixture layer. [b]Turn-on voltage at which emission became detectable. [c]The values of driving voltage and EQE of device at 1000 cd m^{-2}. [d]Maximal external quantum efficiency. [e]Maximal current efficiency. [f]Maximal power efficiency.

Table 1. Both devices show low threshold voltage of 2.0 V for light emission, which is mainly due to direct electron−hole capture at the heterojunction without prior injection of one of the charges into the opposite layer. Device I performed excellently with maximum external quantum (EQE), current (CE), and power (PE) efficiencies of 7.7%, 22.5 cd A^{-1}, and 23.6 lm W^{-1}, respectively. To the best of our knowledge, this device represents the best characteristics of bilayer-type exciplex-based OLEDs. The device (device II) by inserting a TCTA:3P-T2T (1:1) mixture layer exhibited comparable EL efficiencies of 7.8%, 23.6 cd A^{-1}, and 26.0 lm W^{-1} relative to those of device I. However, device II displays higher brightness and current density as well as lower driving voltage (1000 cd m^{-2} at 3.8 eV) as compared to those of device I. The intermolecular contacts between donor and acceptor molecules are enhanced by physically blending them together into a more effective emitting layer, which seems to be beneficial to the EL efficiency. The observed electroluminescence spectra of devices I and II with CIE chromaticity (0.40, 0.55) are the same with the photoluminescence spectrum.

CONCLUSION

In summary, we have demonstrated a record-high (EQE∼7.7%) bilayer-type exciplex-based OLED by using a triazene-centered electron-transporting molecule 3P-T2T as acceptor and a carbazole-based hole-transporting material TCTA as donor. The large offsets of TCTA/3P-T2T energy levels assist the accumulation of charge carriers at the interfacial region for increasing carrier recombination probability to give S_1 and T_1 exciplex excitons. The efficient exciplex formation at TCTA/3P-T2T interfaces is also attributable to the excellent and balanced hole-transporting and electron-transporting properties of TCTA and 3P-T2T, respectively so that sufficient charge carriers are able to reach to the heterojunction. In addition, the high E_Ts values of TCTA and 3P-T2T effectively confine the electro-generated exciplex T_1 state, allowing a RISC process feasible to improve the light-emitting efficiency and hence reach high EL efficiencies. The system (for yellow emission) addressed here provides a prototype. And, in theory, other potential interfacial exciplexes formed between various donor/acceptor interfaces should be feasible and ample. This finding thus paves a new dimension for facile and wide tuning of the exciplex emission throughout the entire visible and even near-IR region.

ASSOCIATED CONTENT

Supporting Information

The AC-2 and UPS data of TCTA and 3P- T2T; absorption (Abs) spectra of TCTA and 3P-T2T neat films as well as TCTA/3P-T2T (1:1) mixed film; experimental details for photophysical measurements, time-of-flight (TOF) mobility measurements, and device fabrications. This material is available free of charge via the Internet at http://pubs.acs.org.

AUTHOR INFORMATION

Corresponding Author

*E-mail: wenhung@mail.ntou.edu.tw; chop@ntu.edu.tw; kenwong@ntu.edu.tw.

Notes

The authors declare no competing financial interest.

ACKNOWLEDGMENTS

This study was supported financially from National Science Council of Taiwan (NSC 100-2112-M-019-002-MY3, 101-2113-M-002-009-MY3, 101-2628-M-002-008) .

REFERENCES

(1) Tang, C. W.; VanSlyke, S. A. *Appl. Phys. Lett.* **1987**, *51*, 913−915.
(2) Kondakov, D. Y. *J. Appl. Phys.* **2007**, *102*, 114504.
(3) Kondakov, D. Y.; Pawlik, T. D.; Hatwar, T. K.; Spindler, J. P. *J. Appl. Phys.* **2009**, *106*, 124510.
(4) King, S. M.; Cass, M.; Pintani, M.; Coward, C.; Dias, F. B.; Monkman, A. P.; Roberts, M. *J. Appl. Phys.* **2011**, *109*, 074502.
(5) Monkman, A. P. *ISRN Mater. Sci.* **2013**, 670130.
(6) Endo, A.; Sato, K.; Yoshimura, K.; Kai, T.; Kawada, A.; Miyazaki, H.; Adachi, C. *Appl. Phys. Lett.* **2011**, *98*, 083302.
(7) Lee, S. Y.; Yasuda, T.; Nomura, H.; Adachi, C. *Appl. Phys. Lett.* **2012**, *101*, 093306.
(8) Tanaka, H.; Shizu, K.; Miyazaki, H.; Adachi, C. *Chem. Commun.* **2012**, *48*, 11392−11394.
(9) Nakagawa, T.; Ku, S.-Y.; Wong, K.-T.; Adachi, C. *Chem. Commun.* **2012**, *48*, 9580−9582.
(10) Zhang, Q.; Li, J.; Shizu, K.; Huang, S.; Hirata, S.; Miyazaki, H.; Adachi, C. *J. Am. Chem. Soc.* **2012**, *134*, 14706−14709.
(11) Uoyama, H.; Goushi, K.; Shizu, K.; Nomura, H.; Adachi, C. *Nature* **2012**, *492*, 234−238.
(12) Tamoto, N.; Adachi, C.; Nagai, K. *Chem. Mater.* **1997**, *9*, 1077−1085.
(13) Wang, J.; Kawabe, Y.; Shaheen, S. E.; Morrell, M. M.; Jabbour, G. E.; Lee, P. A.; Anderson, J.; Armstrong, N. R.; Kippelen, B.; Mash, E. A.; Peyghambarian, N. *Adv. Mater.* **1998**, *10*, 230−233.
(14) Noda, T.; Ogawa, H.; Shirota, Y. *Adv. Mater.* **1999**, *11*, 283−285.
(15) Cocchi, M.; Virgili, D.; Giro, G.; Fattori, V.; Marco, P. D.; Kalinowski, J.; Shirota, Y. *Appl. Phys. Lett.* **2002**, *80*, 2401−2403.
(16) Goushi, K.; Yoshida, K.; Sato, K.; Adachi, C. *Nat. Photon.* **2012**, *6*, 253−258.
(17) Goushi, K.; Adachi, C. *Appl. Phys. Lett.* **2012**, *101*, 023306.
(18) Jankus, V.; Chiang, C.-J.; Dias, F.; Monkman, A. P. *Adv. Mater.* **2013**, *25*, 1455−1459.
(19) Palilis, L. C.; Mäkinen, A. J.; Uchida, M.; Kafafi, Z. H. *Appl. Phys. Lett.* **2003**, *82*, 2209−2211.
(20) Lee, S.; Kim, K.-H.; Limbach, D.; Park, Y.-S.; Kim, J.-J. *Adv. Funct. Mater.* **2013**, DOI: 10.1002/adfm.201300187..
(21) Giebeler, C.; Antoniadis, H.; Bradley, D. D. C.; Shirota, Y. *J. Appl. Phys.* **1999**, *85*, 608−615.
(22) Kawabe, Y.; Abe, J. *Appl. Phys. Lett.* **2002**, *81*, 493−495.
(23) Chao, C.-L.; Chen, S.-A. *Appl. Phys. Lett.* **1998**, *73*, 426−428.
(24) Noda, T.; Ogawa, H.; Shirota, Y. *Adv. Mater.* **1999**, *11*, 283−285.
(25) Matsumoto, N.; Nishiyama, M.; Adachi, C. *J. Phys. Chem. C* **2008**, *112*, 7735−7741.

(26) Su, W. M.; Li, W. L.; Xin, Q.; Su, Z. S.; Chu, B.; Bi, D. F.; He, H.; Niu, J. H. *Appl. Phys. Lett.* **2007**, *91*, 043508.
(27) Carvellia, M.; van Reenen, A.; Janssen, R. A. J.; Loebl, H. P.; Coehoorn, R. *Org. Electron.* **2012**, *13*, 2605−2614.
(28) Chen, H.-F.; Wang, T.-C.; Lin, S.-W.; Hung, W.-Y.; Dai, H.-C.; Chiu, H.-C.; Wong, K.-T.; Ho, M.-H.; Cho, T.-Y.; Chen, C.-W.; Lee, C.-C. *J. Mater. Chem.* **2012**, *22*, 15620−15627.
(29) Lai, S. L.; Chan, M. Y.; Tong, Q. X.; Fung, M. K.; Wang, P. F.; Lee, C. S.; Lee, S. T. *Appl. Phys. Lett.* **2008**, *93*, 143301.
(30) Su, W. M.; Li, W. L.; Xin, Q.; Su, Z. S.; Chu, B.; Bi, D. F.; He, H.; Niu, J. H. *Appl. Phys. Lett.* **2007**, *91*, 043508.
(31) Halls, J. J. M.; Cornil, J.; dos Santos, D. A.; Silbey, R.; Hwang, D. H.; Holmes, A. B.; Bredas, J. L.; Friend, R. H. *Phys. Rev. B* **1999**, *60*, 5721−5727.
(32) Morteani, A. C.; Dhoot, A. S.; Kim, J.-S.; Silva, C.; Greenham, N. C.; Murphy, C.; Moons, E.; Ciná, S.; Burroughes, J. H.; Friend, R. H. *Adv. Mater.* **2003**, *15*, 1708−1712.
(33) Hung, W.-Y.; Ke, T.-H.; Lin, Y.-T.; Wu, C.-C.; Hung, T.-H.; Chao, T.-C.; Wong, K.-T.; Wu, C.-I. *Appl. Phys. Lett.* **2006**, *88*, 064102.
(34) Su, S.-J.; Chiba, T.; Takeda, T.; Kido, J. *Adv. Mater.* **2008**, *20*, 2125−2130.
(35) Su, S.-J.; Takahashi, Y.; Chiba, T.; Takeda, T.; Kido, J. *Adv. Funct. Mater.* **2009**, *19*, 1260−1267.
(36) Matsumoto, N.; Adachi, C. *J. Phys. Chem. C* **2010**, *114*, 4652−4658.